HHS Public Access

Author manuscript

Lab Chip. Author manuscript; available in PMC 2018 January 31.

Published in final edited form as:

Lab Chip. 2017 January 31; 17(3): 395–400. doi:10.1039/c6lc01272h.

Acoustic actuation of bioinspired microswimmers†

Murat Kaynak[a], **Adem Ozcelik**[b], **Amir Nourhani**[c], **Paul E. Lammert**[c], **Vincent H. Crespi**[c], and **Tony Jun Huang**[a,b]

[a]Department of Engineering Science and Mechanics, The Pennsylvania State University, University Park, PA 16802, USA

[b]Department of Mechanical Engineering and Materials Science, Duke University, Durham, NC 27708 USA

[c]Department of Physics, The Pennsylvania State University, University Park, Pennsylvania, 16802 USA

Abstract

Acoustic actuation of bioinspired microswimmers is experimentally demonstrated. Microswimmers are *in situ* fabricated in a microchannel. Upon acoustic excitation, the flagellum of the microswimmer oscillates, which in turn generates linear or rotary movement depending on the swimmer design. The speed of these bioinspired microswimmers is tuned by adjusting the voltage amplitude applied to the acoustic transducer. Simple microfabrication and remote actuation are promising for biomedical applications.

Microswimmers have become increasingly attractive for their potential applications in biological, chemical, and biomedical contexts.[1–10] Thanks to their contactless actuation, artificial microswimmers could carry out various tasks such as targeted drug delivery, particle separation, mixing, pumping, assembly, manipulation, microsurgery, and chemical analysis, often by mimicking the behavior of unicellular biological counterparts.[11–24] Microorganisms or cells such as Escherichia coli (E. coli), human sperm, Chromatium okenii, and Spirillum volutans can propel and steer at low Reynolds number[7,15,21,23,25–27] with oscillating flagella that enable them to find food, reproduce, and escape from danger using helical and sinusoidal modes of actuation, depending on the ambient medium.[6,27–32] New classes of useful artificial microswimmers which are inspired by these natural designs will be particularly valuable if they can be achieved with simple and efficient means of fabrication and actuation.

Microswimmers can autonomously propel by interacting with electrical,[33] chemical,[9] magnetic,[8,12,16,28,34,35] or acoustic[1,4,14,36–40] fields, or combinations thereof.[13,38] For example, a uniform electric field can create an imbalance in electrochemical activity along the motor axis and thus induce motility[33,42] with a velocity controlled by the applied

†Electronic Supplementary Information (ESI) available: Figure S1: Oscillation amplitude analysis of rotational microswimmer. Video 1: Flagellum oscillation. Video 2: Microswimmer without flagellum. Video 3: Directional motility. Video 4: Opposite rotation. Video 5: Swimming towards each other. Video 6: Microswimmer changes directions Video 7: Single rotation. See DOI: 10.1039/x0xx00000x

Correspondence to: Vincent H. Crespi; Tony Jun Huang.

electric field. Other microswimmers are powered by asymmetric consumption of chemical fuels such as hydrogen peroxide that is driven by compositional and/or structural asymmetries in the swimmer.[9] Microswimmers with magnetic elements can be driven and/or steered by interaction with an external magnetic field, with good speed and directional control.[9,12,16,28,34,35] Acoustically driven microswimmers use acoustic streaming[43–47]and radiation forces[43,48–52] to swim in various liquid environments.[1,4,14,36–38] Combinations of the above methods have been realized to achieve greater functionality, such as chemical-plus-acoustic propulsion for axial direction and speed control,[41] or magnetic-plus-acoustic fields to acoustically propel and magnetically steer nanowire motors.[14] Despite these advances in microswimmer fabrication and actuation, there is still a need for biocompatible microswimmers that are remotely and noninvasively powered.[53]

Acoustic propulsion is biocompatible and largely medium-independent, and thus is an appropriate candidate to power microswimmers noninvasively.[54–56] Here we demonstrate *in situ* fabrication and acoustic actuation of bioinspired microswimmers within a microchannel. Their design is inspired by flagellated organisms, although they operate at a higher frequency: the artificial flagellum is driven into oscillation by an external acoustic field and thus generates acoustically driven streaming[57], which in turn creates a variety of contactless and fuel-free swimming behaviors such as directional locomotion and rotation. These microswimmers are easy to fabricate, biocompatible, and remotely powered.

In order to prepare the set up as shown in Fig. 1, we first fabricated a replica mold by soft lithography using a silicon master. For the master fabrication, a 4-inch-diameter silicon wafer pretreated with hexamethyldisilazane was patterned in a photoresist (Megaposit SPR955, Microchem, USA) and etched using deep reactive ion etching. The silicon wafer was then vapor-coated with chlorotrimethylsilane (75-77-4, Alfa Aesar, USA) to ease the peeling of PDMS channel from. PDMS resin and curing agent (Sylgard 184, Dow-Corning, USA) were mixed in a 10:1 ratio, and this mixture was poured onto the silicon master in a petri dish and baked at 65°C for 2 h. Next we removed the cured PDMS and punched the inlet and outlet holes using a biopsy punch (Harris Uni-Core 0.75 mm). We used a glass slide (48404–454, VWR, USA) as the substrate. The glass slide was first coated with the PDMS mixture using a spin coater (WS-650MZ-23NPP/Lite, Laurell Technologies, Czech Republic) at 1000 RPM for 1 minute. Then the PDMS-coated glass slide was baked at 65°C for 30 minutes. The PDMS-coated glass slide and PDMS microchannel surfaces were activated by a high-frequency generator (BD-10AS, Electro-Technic Products, USA). Then the PDMS-coated glass slide and the microchannel were bonded at 65°C overnight.

For the miscroswimmer fabrication, we injected a solution of 40% (v/v) polyethylene glycol (PEG) diacrylate with a molecular weight of 700 (PEG700, Sigma-Aldrich, MO, USA), 30% (v/v) PEG with a molecular weight of 258 (PEG 258, Sigma-Aldrich, MO, USA), 15% (v/v) photo-initiator 2-Hydroxy-2-methyl-1-phenyl-propan-1-one (Darocur 1173, from Ciba), and 15% (v/v) TE buffer (100 TE, from OmniPur) into the inlet through polythene tubing (Product code:10793527, Smith’s Medical, USA). An inverted microscope equipped with 10X objective lens (Plan Fluor 10x/0.3 DIC L/N1, infinity/0.17 WD 16.0, Nikon, Japan), a filter cube (11000v3: UV, Chroma), and a mercury lamp (Intensilight C-HGFI,

Nikon, Japan), was used to fabricate microswimmers *in situ*. A photomask with the design of the microswimmers was inserted at the field-stop of the microscope before the objective lens. The UV exposure time of 50 ms was controlled by a computer-controlled mechanical shutter (LB-SC, Sutter Instrument Company, CA, USA). We measured the UV light intensity as ~80 μW/cm^2 before the light entered the microchannel by a power meter (FieldMaxII-TO Laser Power/Energy Meter, Coherent Inc., USA). After being patterned by the photomask, UV light was focused by a 10x objective lens and entered the microchannel from below. It polymerized the solution throughout the channel height, excepting a thin (1–3 μm) oxygen inhibition layer at the bottom and top of the microchannel (PDMS is an oxygen-permeable material[58]). This layer ensures freely moving microswimmers after we wash the un-polymerized solution with ethanol.

We glued a piezoelectric transducer (81-7BB-27-4L0, Murata Electronics, Japan) next to the PDMS microchannel using epoxy (G14250, MA, USA). This piezoelectric transducer is the source of acoustic streaming via vibration.[59,60] A signal generator (AFG3011, Tektronix, USA) and a radio-frequency power amplifier (25A250A, Amplifier Research, USA) generate a sine wave to actuate the transducer.

Fig. 1 provides a schematic for the *in situ* fabrication of a linear microswimmer that is ~180 μm long, ~60 μm wide (at the head of the swimmer), and ~45 μm tall. A photocurable solution inside a microchannel is UV polymerized into the shape of a photomask that has been placed in the field-stop of an inverted microscope (Fig. 1b). Microswimmers are fabricated in a single ~50 millisecond step, in contrast to prior labor-intensive multistep fabrication schemes.[14,33,39] The polymer we use is biocompatible and can accommodate various useful payloads such as nanoparticles, cells, or drugs. The tail of the microswimmer oscillates at much higher amplitude than the head, due to its greater flexibility (Video 1, Supporting Information). Tail oscillation generates acoustic streaming flows due to viscous damping; we previously reported extensive numerical analyses of this phenomenon for various types of oscillating structures.[57,61,62] These acoustically driven streaming flows presumably propel the microswimmer, in a direction opposite the streaming (Fig. 1c). Note a distinction here from biological flagella, which operate at much lower frequencies.

Fig. 2 shows four artificial polymer structures of different designs. As a control case, we first fabricated “swimmers” without flagella (Fig. 2a and b). Under the acoustic field, these microstructures do not swim (Video 2, Supporting Information). The next design is a linear microswimmer whose head and tail are inspired by flagellated microorganisms (Fig. 2c and d). As expected, the flagellum oscillates and induces directional motion along the head-tail axis (Video 3, Supporting Information). By breaking reflection symmetry about the swimmer’s midline, we can also obtain rotational microswimmers that, within the confinement of the microchannel (which prevents the swimmer from flipping over), are pre-programmed for clockwise or counter-clockwise rotation according to which side of the structure hosts the flagellum, as shown in Fig. 2e–h and Video 4 in Supporting Information.

Two microswimmers of opposite structural chirality rotate in opposite directions under the same acoustic field, demonstrating that the sense of rotation is controlled by the swimmer chirality rather than characteristics of the acoustic field. Similarly, two linear

microswimmers of similar design can move directly towards each other, as shown in Fig. 3, proving that swimming is due to local swimmer orientation, not bulk fluid motion. In Fig. 3a, these microswimmers are motionless in the absence of acoustic excitation. After application of an external acoustic field, each swims directly towards the other at ~600 μm/s (Fig. 3b). After a slightly glancing collision, the swimmers pass each other and continue along their original directions of motion, as shown in Video 5 of Supporting Information. Frequency response of microrotors with similar sharp edge structures in the same experimental setup was analyzed in our previous work.[57] Similarly, the maximum speeds for both linear and rotational motion were obtained in the vicinity of the resonant frequency of the transducer, 4.6±0.5 kHz. Outside of this range performance degraded rapidly, presumably due to fall-off in the performance of the transducer. Nevertheless, swimming direction of the linear microswimmers with two additional side branches was also affected by changing the frequency. This behavior may be explained by the frequency-dependent variation of the oscillation profile of the glass slide (Video 6 and Fig. S2, Supporting Information)[44]. However, in order to better understand and utilize this behavior, we need to conduct further experimental and theoretical analyses.

The amplitude of the flagellar oscillation seen in Fig. 4a–d is monotonic in the amplitude of the applied acoustic field (controlled by the voltage amplitude at the amplifier), which enables fine control of the microswimmer speed. Fig. 4e shows the terminal velocity of the flagellated directional microswimmers as a function of the peak-to-peak voltage (V_{PP}) applied to the transducer. In contrast with prior acoustically powered microrotors that were rotated about fixed axles,[57] there is no zero-offset in the voltage required to initiate motion – we ascribe this improved performance to a lack of frictional interactions with nearby supporting structures in these free swimmers (in contrast to the fixed axles present in the prior microrotors). The dependence of speed on drive voltage is slightly supra-linear, which may arise from nonlinearities in the flagellar oscillations at the highest drive amplitudes (see below).

Fig. 4a–d show an image series for the motion of a linear microswimmer driven at 100 V_{PP}. The terminal speed is ~200 μm/s at 20 V_{PP}, increasing to ~1200 μm/s at 140 V_{PP} (stronger actuation than this leads to very rapid motion that is difficult to quantitatively characterize in the current experimental setup). The linear swimmers can be potentially used in applications such as targeted drug delivery. During UV polymerization, drugs can be trapped in the microswimmer, transported to a specific location, and released via an external stimulus.

Similarly, Fig. 5 shows the relationship of angular speed to V_{PP} for rotational microswimmers. In Fig. 5a, the flagellum is at rest in the absence of acoustic excitation. It then begins to oscillate and rotate the body of the swimmer when the acoustic transducer is activated, as shown in Video 7 of Supporting Information. Based on the large amplitude of the observed deformations, the flagellum likely enters a nonlinear regime at the largest-amplitude excitations. Fig. 5a–f shows a full counter-clockwise rotation at 140 V_{PP}. The angular speed increases with increasing V_{PP}, again supra-linearly at the largest amplitudes, as shown in Fig. 5g. The angular speed is ~25 RPM at 20 V_{PP}, increasing to about 200 RPM at 140 V_{PP}; the corresponding linear speed at the outer edge of the rotary swimmer is comparable to the translational speed of the linear swimmer at a similar drive voltage. These

voltages correspond to oscillation amplitudes of the tail varying from ~12 to ~40 μm (Fig. S1, Supporting Information). Different microswimmer geometries that also break reflection symmetry but reduce viscous drag on the body of the swimmer could potentially achieve higher rotation rates.

Conclusions

We have demonstrated *in situ* fabrication and acoustic actuation of flagellated rotational and linear microswimmers which are inspired by flagellated biological microswimmers. For the former, sustained clockwise or counterclockwise rotation can be maintained by using swimmers that are resistant to flipping over within the microchannel. For the latter, we designed microswimmers with a head and a tail which is inspired by the geometry of a bacterial flagellum. The flagella oscillate under acoustic field and thus generate acoustically driven streaming that drives the microswimmers. The linear microswimmers reach ~1200 μm/s, while rotational microswimmers rotate at 200 RPM. The simple, durable, biocompatible, and inexpensive fabrication and remote actuation of these biologically inspired microswimmers show potential for various applications in physics, biochemistry, and biomedical engineering, such as targeted drug delivery, fluid manipulation, micro assembly, cell manipulation, microsurgery, and chemical analysis.

Supplementary Material

Refer to Web version on PubMed Central for supplementary material.

Acknowledgments

We gratefully acknowledge financial support from the National Institutes of Health (R01 GM112048 and R33 EB019785), the National Science Foundation (IIP-1534645, CBET-1438126, IDBR-1455658), and the Penn State MRSEC Center for Nanoscale Science under grant DMR-1420620). This work was completed in the Penn State University Materials Research Institute Nanofab Facility. Murat Kaynak and Adem Ozcelik acknowledge the support from Turkey's Ministry of National Education.

References

1. Ahmed D, Lu M, Nourhani A, Lammert PE, Stratton Z, Muddana HS, Crespi VH, Huang TJ. Sci Rep. 2015; 5:9744. [PubMed: 25993314]
2. Mijalkov M, Volpe G. Soft Matter. 2013; 9:6376.
3. Grosjean G, Lagubeau G, Darras A, Hubert M, Lumay G, Vandewalle N. Sci Rep. 2015; 5:16035. [PubMed: 26538006]
4. Bertin N, Spelman TA, Stephan O, Gredy L, Bouriau M, Lauga E, Marmottant P. Phys Rev Appl. 2015; 4:64012.
5. Volpe G, Buttinoni I, Vogt D, Kümmerer HJ, Bechinger C. Soft Matter. 2011; 7:8810.
6. Yan X, Zhou Q, Yu J, Xu T, Deng Y, Tang T, Feng Q, Bian L, Zhang Y, Ferreira A, Zhang L. Adv Funct Mater. 2015; 25:5333.
7. Stanton MM, Trichet-Paredes C, Sánchez S. Lab Chip. 2015; 15:1634. [PubMed: 25632887]
8. Carlsen RW, Edwards MR, Zhuang J, Pacoret C, Sitti M. Lab Chip. 2014; 14:3850. [PubMed: 25120224]
9. Simmchen J, Katuri J, Uspal WE, Popescu MN, Tasinkevych M, Sánchez S. Nat Commun. 2016; 7:10598. [PubMed: 26856370]

10. Agarwal AK, Sridharamurthy SS, Beebe DJ, Jiang Hongrui. J Microelectromechanical Syst. 2005; 14:1409.
11. Zhang L, Peyer KE, Nelson BJ. Lab Chip. 2010; 10:2203. [PubMed: 20567752]
12. Peyer KE, Zhang L, Nelson BJ. Nanoscale. 2013; 5:1259. [PubMed: 23165991]
13. Carlsen RW, Sitti M. Small. 2014; 10:3831. [PubMed: 24895215]
14. Ahmed S, Wang W, Mair LO, Fraleigh RD, Li S, Castro LA, Hoyos M, Huang TJ, Mallouk TE. Langmuir. 2013; 29:16113. [PubMed: 24345038]
15. Stanton MM, Simmchen J, Ma X, Miguel-López A, Sánchez S. Adv Mater Interfaces. 2016; 3 n/a.
16. Lu, Liang-Hsuan, Ryu, Kee Suk, Liu, Chang. J Microelectromechanical Syst. 2002; 11:462.
17. Gao W, Wang J. Nanoscale. 2014; 6:10486. [PubMed: 25096021]
18. Wang W, Duan W, Sen A, Mallouk TE. Proc Natl Acad Sci. 2013; 110:17744. [PubMed: 24127603]
19. Wang W, Duan W, Ahmed S, Sen A, Mallouk TE. Acc Chem Res. 2015; 48:1938. [PubMed: 26057233]
20. Ahmed S, Gentekos DT, Fink CA, Mallouk TE. ACS Nano. 2014; 8:11053. [PubMed: 25247764]
21. Elgeti J, Winkler RG, Gompper G. Reports Prog Phys. 2015; 78:56601.
22. Katuri J, Seo KD, Kim DS, Sánchez S. Lab Chip. 2016; 16:1101. [PubMed: 26882472]
23. Nosrati R, Driouchi A, Yip CM, Sinton D. Nat Commun. 2015; 6:8703. [PubMed: 26555792]
24. Zhu W, Li J, Leong YJ, Rozen I, Qu X, Dong R, Wu Z, Gao W, Chung PH, Wang J, Chen S. Adv Mater. 2015; 27:4411.
25. Wang W, Duan W, Ahmed S, Mallouk TE, Sen A. Nano Today. 2013; 8:531.
26. Qiu T, Lee TC, Mark AG, Morozov KI, Münster R, Mierka O, Turek S, Leshansky AM, Fischer P. Nat Commun. 2014; 5:5119. [PubMed: 25369018]
27. Jikeli JF, Alvarez L, Friedrich BM, Wilson LG, Pascal R, Colin R, Pichlo M, Rennhack A, Brenker C, Kaupp UB. Nat Commun. 2015; 6:7985. [PubMed: 26278469]
28. Peyer KE, Tottori S, Qiu F, Zhang L, Nelson BJ. Chem - A Eur J. 2013; 19:28.
29. Purcell EM. Am J Phys. 1977; 45:3.
30. Lauga E, Powers TR. Reports Prog Phys. 2009; 72:96601.
31. Lauga E, Eloy C. J Fluid Mech. 2013; 730:R1.
32. Higdon JJL. J Fluid Mech. 1979; 90:685.
33. Loget G, Kuhn A. Nat Commun. 2011; 2:535. [PubMed: 22086336]
34. Dhar P, Cao Y, Kline T, Pal P, Swayne C, Fischer TM, Miller B, Mallouk TE, Sen A, Johansen TH. J Phys Chem C. 2007; 111:3607.
35. Ghosh A, Fischer P. Nano Lett. 2009; 9:2243. [PubMed: 19413293]
36. Wang W, Li S, Mair L, Ahmed S, Huang TJ, Mallouk TE. Angew Chemie. 2014; 126:3265.
37. Chen Y, Ding X, Steven Lin S-C, Yang S, Huang P-H, Nama N, Zhao Y, Nawaz AA, Guo F, Wang W, Gu Y, Mallouk TE, Huang TJ. ACS Nano. 2013; 7:3306. [PubMed: 23540330]
38. Feng J, Yuan J, Cho SK. Lab Chip. 2015; 15:1554. [PubMed: 25650274]
39. Ahmed D, Baasch T, Jang B, Pané S, Dual J, Nelson BJ. Nano Lett. 2016 acs.nanolett.6b01601.
40. Jonathan, D Kao, John, Warren, Jie, Xu, Attinger. 2006 NSTI Nanotechnol. Conf. Trade Show - NSTI Nanotech 2006 Tech. Proc; 2006; p. 4
41. Wang W, Duan W, Zhang Z, Sun M, Sen A, Mallouk TE. Chem Commun. 2015; 51:1020.
42. Eamer L, Nosrati R, Vollmer M, Zini A, Sinton D. Biomicrofluidics. 2015; 9:44113.
43. Ahmed D, Ozcelik A, Bojanala N, Nama N, Upadhyay A, Chen Y, Hanna-Rose W, Huang TJ. Nat Commun. 2016; 7:11085. [PubMed: 27004764]
44. Ozcelik A, Nama N, Huang PH, Kaynak M, McReynolds MR, Hanna-Rose W, Huang TJ. Small. 2016; 12:5120. [PubMed: 27515787]
45. Huang PH, Xie Y, Ahmed D, Rufo J, Nama N, Chen Y, Chan CY, Huang TJ. Lab Chip. 2013; 13:3847. [PubMed: 23896797]
46. Ahmed D, Chan CY, Lin S-CS, Muddana HS, Nama N, Benkovic SJ, Jun Huang T. Lab Chip. 2013; 13:328. [PubMed: 23254861]

47. Huang PH, Nama N, Mao Z, Li P, Rufo J, Chen Y, Xie Y, Wei CH, Wang L, Huang TJ. Lab Chip. 2014; 14:4319. [PubMed: 25188786]
48. Guo F, Li P, French JB, Mao Z, Zhao H, Li S, Nama N, Fick JR, Benkovic SJ, Huang TJ. Proc Natl Acad Sci. 2015; 112:43. [PubMed: 25535339]
49. Guo F, Mao Z, Chen Y, Xie Z, Lata JP, Li P, Ren L, Liu J, Yang J, Dao M, Suresh S, Huang TJ. Proc Natl Acad Sci. 2016; 113:1522. [PubMed: 26811444]
50. Chen Y, Li S, Gu Y, Li P, Ding X, Wang L, McCoy JP, Levine SJ, Huang TJ. Lab Chip. 2014; 14:924. [PubMed: 24413889]
51. Chen Y, Nawaz AA, Zhao Y, Huang PH, McCoy JP, Levine SJ, Wang L, Huang TJ. Lab Chip. 2014; 14:916. [PubMed: 24406848]
52. Ding X, Shi J, Lin SCS, Yazdi S, Kiraly B, Huang TJ. Lab Chip. 2012; 12:2491. [PubMed: 22648600]
53. Yeh J-LA, Jiang Hongrui, Neves HP, Tien NC. J Microelectromechanical Syst. 2000; 9:281.
54. Qiu Y, Wang H, Demore C, Hughes D, Glynne-Jones P, Gebhardt S, Bolhovitins A, Poltarjonoks R, Weijer K, Schönecker A, Hill M, Cochran S. Sensors. 2014; 14:14806. [PubMed: 25123465]
55. Austin Suthanthiraraj PP, Piyasena ME, Woods TA, Naivar MA, López GP, Graves SW. Methods. 2012; 57:259. [PubMed: 22465280]
56. Marina OC, Sanders CK, Kaduchak G, Goddard GR, Graves SW. Anal Methods. 2011; 3:2573.
57. Kaynak M, Ozcelik A, Nama N, Nourhani A, Lammert PE, Crespi VH, Huang TJ. Lab Chip. 2016; 16:3532. [PubMed: 27466140]
58. Dendukuri D, Pregibon DC, Collins J, Hatton TA, Doyle PS. Nat Mater. 2006; 5:365. [PubMed: 16604080]
59. Xu, J., Attinger, D. Encycl Microfluid Nanofluidics. Springer US; Boston, MA: 2013. p. 1-10.
60. Qiu Y, Gigliotti J, Wallace M, Griggio F, Demore C, Cochran S, Trolier-McKinstry S. Sensors. 2015; 15:8020. [PubMed: 25855038]
61. Nama N, Huang PH, Huang TJ, Costanzo F. Lab Chip. 2014; 14:2824. [PubMed: 24903475]
62. Nama N, Barnkob R, Mao Z, Kähler CJ, Costanzo F, Huang TJ. Lab Chip. 2015; 15:2700. [PubMed: 26001199]

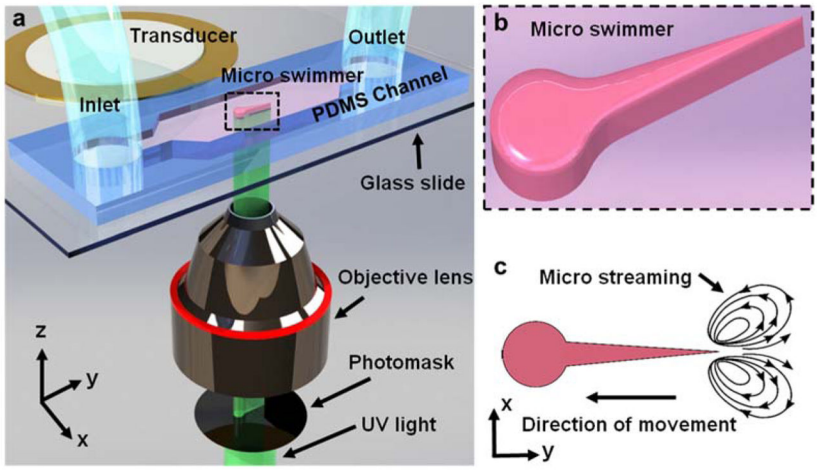

Fig. 1.

Fabrication and acoustic actuation of microswimmers. (a) Fabrication and actuation setup. UV light is patterned and focused by photomask and objective lens. (b) Schematic of microswimmer which is *in situ* fabricated and moves freely. (c) Schematic of microstreaming at the tip of flagellated tail. The microstreaming, which originates from oscillation of the flagellated tail, propels the microswimmer.

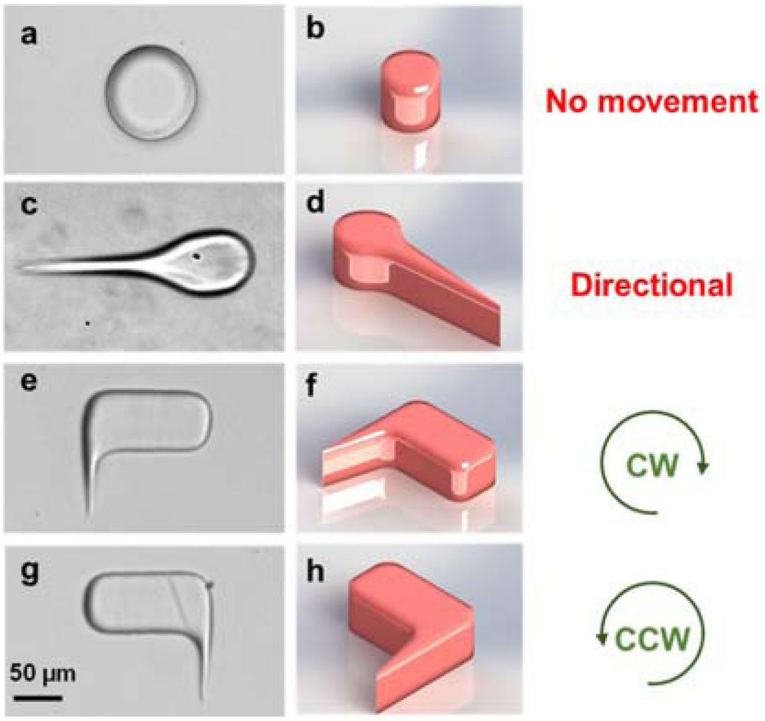

Fig. 2.

Design of different microswimmers. (a) and (b): image and schematic of a microstructure which is not able to rotate. (c) and (d): microswimmer moves directionally due to acoustic streaming. (e) and (f): the oscillation of flagella creates clockwise rotation due to unsymmetrical design. (g) and (h): microswimmer rotates counter-clockwise.

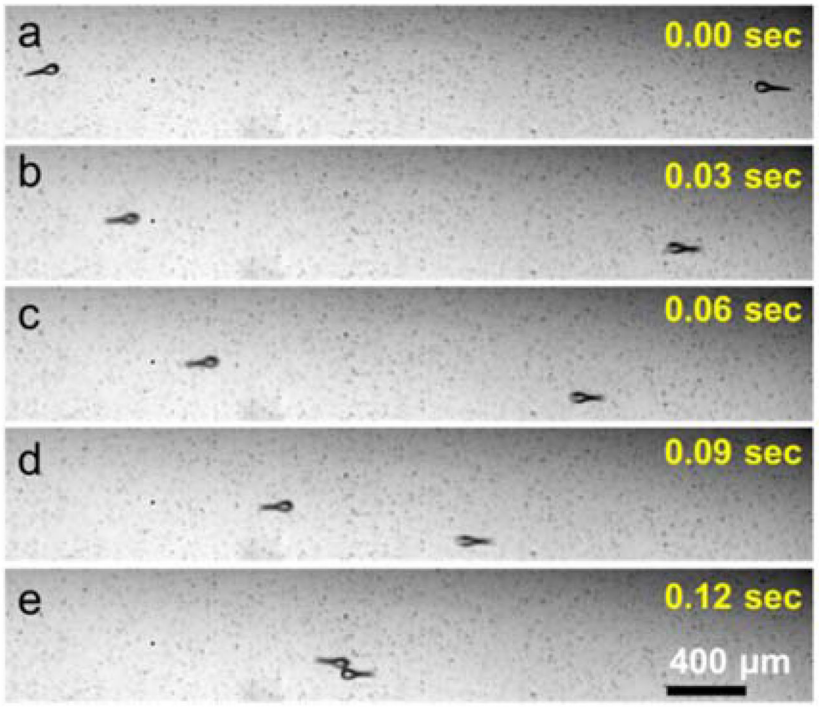

Fig. 3.

Opposing movement of microswimmers under the same conditions. (a) Both microswimmers are at rest, absent any oscillations of their flagella due to the lack of acoustic actuation. (b), (c), (d) and (e) Microswimmers move in opposite directions under 140 V_{PP} acoustic excitation. (See supplementary video).

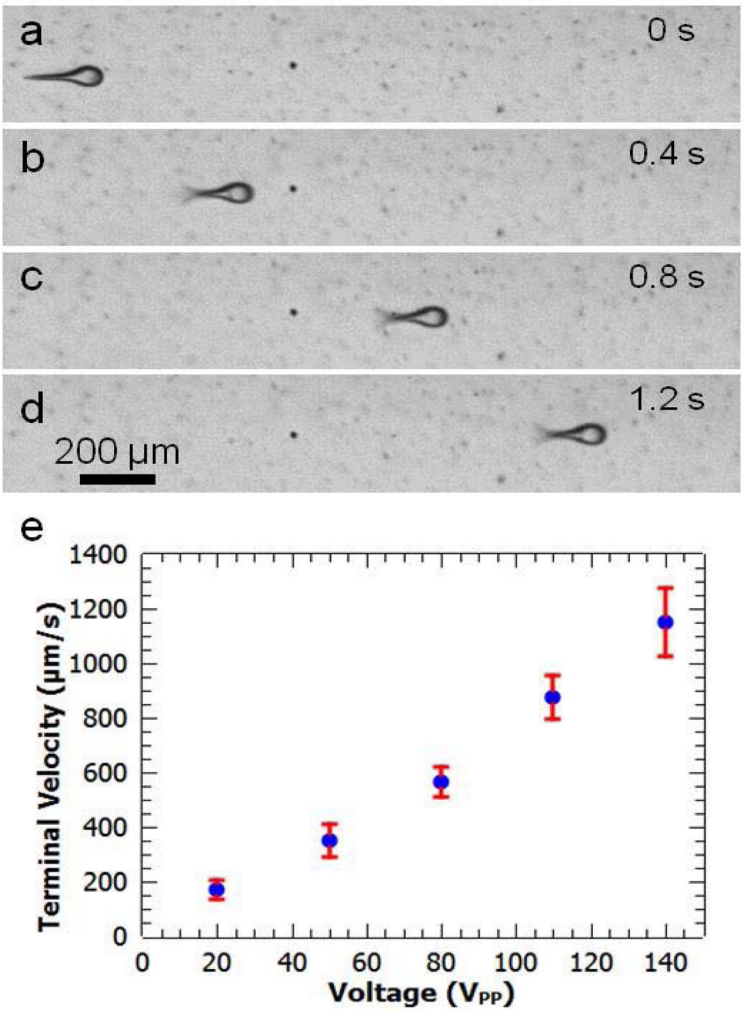

Fig. 4.

Characterization of microswimmers' directional movement. (a) Microswimmer is stationary in the absence of acoustic oscillation. (b) Actuating the PZT transducer at 140 VPP, the microswimmer's flagella oscillates and it moves directionally. (c) and (d): Under constant excitation voltage (140 VPP), the microswimmer moves at a constant velocity. (e) The terminal velocity of a microswimmer as a function of voltage, increasing from 220 µm/s at 20 VPP to 1200 µm/s at 140 VPP.

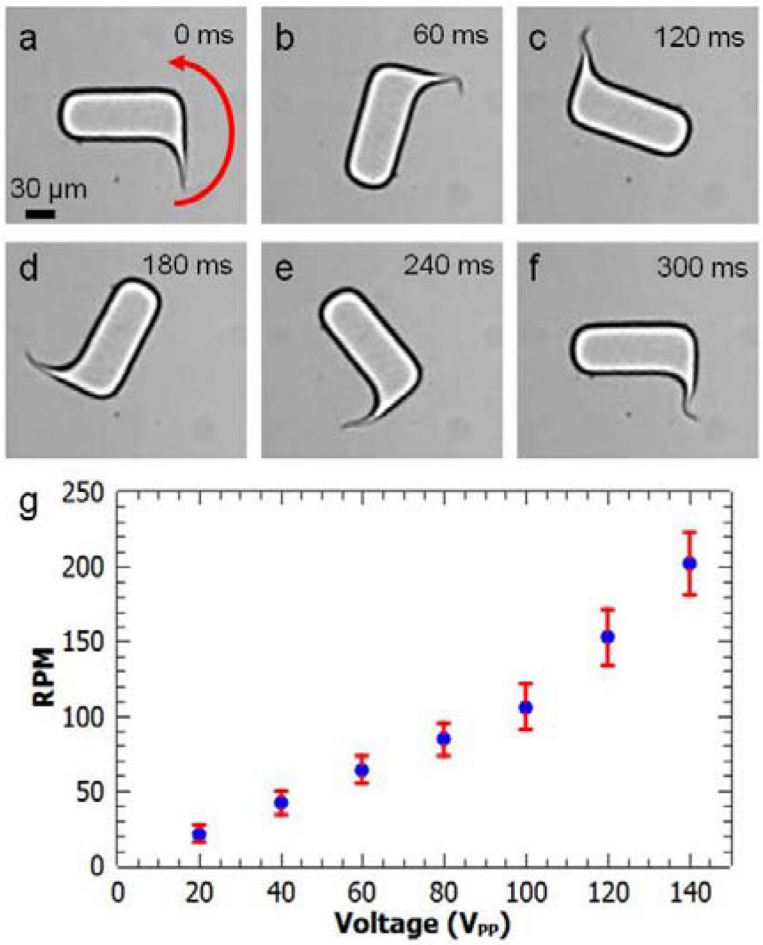

Fig. 5.

Microswimmer's rotational movement. (a)–(f): A full revolution divided into six frames, at 140 V_{pp} excitation. (e) The angular speed as a function of voltage, increasing from 25 RPM at 20 V_{pp} to 200 RPM at 140 V_{pp}.